J Fluoresc (2014) 24:579–588
DOI 10.1007/s10895-013-1330-7

ORIGINAL PAPER

Interaction of Sulfadiazine with Model Water Soluble Proteins: A Combined Fluorescence Spectroscopic and Molecular Modeling Approach

Mullah Muhaiminul Islam · N. Shaemningwar Moyon · Pynsakhiat Miki Gashnga · Sivaprasad Mitra

Received: 19 August 2013 / Accepted: 20 November 2013 / Published online: 28 November 2013

Abstract The binding behavior of antibacterial drug sulfadiazine (SDZ) with water soluble globular proteins like bovine as well as human serum albumin (BSA and HSA, respectively) and lysozyme (LYS) was monitored by fluorescence titration and molecular docking calculations. The experimental data reveal that the quenching of the intrinsic protein fluorescence in presence of SDZ is due to the strong interaction in the drug binding site of the respective proteins. The Stern-Volmer plot shows positive deviation at higher quencher concentration for all the proteins and was explained in terms of a sphere of action model. The calculated fluorophore-quencher distances vary within 4~11 Å in different cases. Fluorescence experiments at different temperature indicate thermodynamically favorable binding of SDZ with the proteins with apparently strong association constant (~10^4–10^5 M^{-1}) and negative free energy of interaction within the range of −26.0~ −36.8 kJ mol^{-1}. The experimental findings are in good agreement with the respective parameters obtained from best energy ranked molecular docking calculation results of SDZ with all the three proteins.

Keywords Serum albumin · Lysozyme · Sulfadiazine · Tryptophan fluorescence quenching · Hydrophobic interaction · Molecular docking

Electronic supplementary material The online version of this article (doi:10.1007/s10895-013-1330-7) contains supplementary material, which is available to authorized users.

M. M. Islam · N. S. Moyon · P. M. Gashnga · S. Mitra (✉)
UGC Center for Advanced Studies, Department of Chemistry, North-Eastern Hill University, Shillong 793 022, India
e-mail: smitra@nehu.ac.in

S. Mitra
e-mail: sivaprasadm@yahoo.com

Introduction

Sulfadiazine (4-amino-N-pyrimidin- 2-yl-benzenesulfonamide, SDZ) is a short-acting anti-bacterial drug of the parent sulfonamide class of synthetic antibiotic compounds. It eliminates bacteria that cause infections by stopping the production of folate inside the bacterial cell, and is commonly used to treat urinary tract infections (UTIs) [1]. Also SDZ, in combination with an anti-malarial drug pyrimethamine, is frequently used to treat toxoplasmosis in warm-blooded animals like immunocompromised HIV-positive individual patients [2].

The therapeutic use of sulfonamide antibiotics is restricted in veterinary field because of the health risk associated with consumption of sulfonamide residue contaminated animal products [3, 4]. Furthermore, hypersensitive patients who suffer a reaction after taking a sulfonamide drug are thought to be at increased allergic risk for other drugs as well [5], although the mechanism of sulfonamide-related reactions is poorly understood till date. Also, exposure to sulfonamide residues to the consumers for prolonged period is known to cause the development of drug-resistant bacteria [6]. Keeping these in mind, we have investigated the mechanism of interaction of SDZ with model water soluble proteins like bovine as well as human serum albumins (BSA and HSA, respectively) and lysozyme (LYS) by fluorescence quenching method.

Quenching measurement of intrinsic protein fluorescence is an important method to investigate the interactions of drugs with proteins. It can reveal the accessibility of quenchers to albumin's fluorophore groups, mainly tryptophan (trp) and/or tyrosin (tyr), and helps to understand the binding mechanism of albumins with drugs and provide clues to the essential of binding phenomenon. In this work, BSA, HSA and LYS are selected as the model proteins because of their medicinal importance, low cost, commercial availability, and unusual ligand-binding properties [7–9]. BSA is 66 kDa protein

containing two tryptophan residues that possess intrinsic fluorescence, trp212 is located within a hydrophobic binding pocket of the protein and trp134 is located on the surface of the molecule [10–12]. The structural homologue HSA is a protein with the molecular weight of 66,500 containing 585 amino acid residues. However, there is only a single trp residue within HSA at the position of 214 in domain II, which makes it very convenient to study the protein intrinsic fluorescence [13–15]. On the other hand, lysozyme is an antimicrobial protein widely distributed in various biological fluids and tissues including avian egg and animal secretions, human milk, tears, saliva, airway secretions, and secreted by polymorphonuclear leukocytes [16]. It has many physiological and pharmaceutical functions, such as anti-inflammatory, antiviral, immune modulatory, anti-histaminic and anti-tumor activities [17–21]. So it is extensively used in the pharmaceutical and food fields. Intriguingly, LYS also has the capacity to carry drugs and it can cure some illness via the binding with these drugs. It is a 14.6 kDa single chain protein and is formed by 129 amino acid residues, including α-helix, β-sheet, turns and disorder. It contains six trp residues, four disulfide bonds and three tyrosine molecules in its structure [22–24]. Three of the trp residues are located at the substrate binding sites, two in the hydrophobic matrix box, while one is separated from the others [25]. Among the amino acid residues trp62 and trp108 are the most dominant fluorophores, both being located at the substrate binding sites [26].

In view of the multifarious functions of BSA, HSA as well as LYS and their important practical role from a medicinal point of view, studies on the interactions between drugs and these proteins have important meaning on realizing the transport and metabolism process of the drugs, the relationship of structure and function of proteins, and the chemical essence of the interaction between biological macromolecule with small molecule. In this contribution, we report the interaction of SDZ with these three water soluble proteins by steady state and time-resolved fluorescence quenching method. Nonlinear variation in fluorescence quenching data at higher SDZ concentration was modeled by quenching sphere of action mechanism. Finally, the thermodynamic parameters, nature of forces responsible for drug binding and location of the probe in macromolecular architecture were discussed based on the results of temperature variation experiments as well as molecular docking studies.

Materials & Methods

Materials

Sulfadiazine (SDZ) powder of purity ≥ 99 % was purchased from Sigma—Aldrich Chemical Company. Essentially fatty acid and globulin free, >99 % (agarose gel electrophoresis), lyophilized powder form of BSA and HSA were used as obtained from Sigma and USB Corp. USA, respectively. Chicken egg white LYS, also from USB Corp. USA, was used as received. For making the buffer solution the analytical grade type II water (resistivity ~10 MΩ.cm at room temperature) was obtained from Elix 10 water purification system (Millipore India Pvt. Ltd.), crystalline form of Tris(hydroxymethyl)aminomethane hydrochloride (Trizma-HCl) was procured from Sigma-Aldrich Chemical Pvt and extra-pure analytical grade of sodium hydroxide pellets were received from Sisco Research Laboratories (SRL), India. The samples were dissolved in Trizma-HCl buffer solution (0.05 M Trizma-HCl and 0.12 M NaOH,) of pH=7.4. The solution pH was checked with Systronics μ-pH system 361. The protein concentration in all cases was maintained at ~12 μM; whereas, SDZ concentration was varied from 0 to 0.242 mM in all the experiments. The freshly prepared solution mixtures were kept about half an hour for settling before the spectroscopic measurements.

Apparatus & Methods

The experimental methods and data analysis procedure is essentially same as that described elsewhere [27, 28]. Briefly, steady state absorption measurements were performed in a Perkin-Elmer model Lambda25 absorption spectrophotometer. Fluorescence spectral measurements in case of LYS-SDZ system was taken in Hitachi FL-4500 spectrofluorimeter; whereas for BSA and HSA, Quanta Master (QM-40) steady state apparatus obtained from Photon Technology International (PTI) was used. All the spectra were corrected for the instrument response function. For fluorescence emission, the sample was excited at 295 nm unless otherwise mentioned, whereas excitation spectra were obtained by monitoring at the respective emission maximum. In case of LYS experiment 2.5/5.0 nm excitation/emission band pass were used to collect the fluorescence emission. The corresponding parameters for BSA and HSA experiments were 0.2/3 and 0.2/5 nm, respectively. All the measured spectra were subtracted off from the corresponding sample blanks measured under identical condition. Although SDZ have insignificant absorption at the trp excitation wavelength used in this study (295 nm), each fluorescence spectrum (F) of the protein in presence of different ligand concentration was corrected for any possible inner filter effect using the following equation [27].

$$F^{corr}(\lambda_E, \lambda_F) = F(\lambda_E, \lambda_F) \times \frac{A(\lambda_E)}{A_{tot}(\lambda_E)} \quad (1)$$

Where, A represents the absorbance of the free protein, and A_{tot} is the total absorbance of the solution at the excitation wavelength (λ_E). The corrected spectrum can be taken as the contribution only from the protein trp residue. The

corresponding steady-state data, thus obtained from three separate experiments, were averaged and further analyzed using Origin 6.0 (Microcal Software, Inc., USA). The temperature variation experiments were carried out by attaching a circulatory thermostat bath (MLW, Germany, type U2C) to the cell holder.

The fluorescence decay curves were obtained by using 295 nm LED excitation in a PicoMaster time correlated single photon counting (TCSPC) lifetime apparatus (PM-3) supplied by PTI. The instrument response function (IRF) was obtained by using a dilute colloidal suspension of dried non-dairy coffee whitener. The experimentally obtained fluorescence decay traces I(t), collected at the magic angle (54.7°) to eliminate any contribution from the anisotropy decay, were expressed as a sum of exponentials (Eq. (2)) and analyzed by non–linear least–square iterative convolution method based on Lavenberg–Marquardt [29] algorithm as implemented in the data analysis software (Felix GX version 4.0.3) from PTI.

$$F(t) = \sum\nolimits_i \alpha_i exp\left(\frac{-t}{\tau_i}\right) \quad (2)$$

where, α_i is the amplitude of the ith component associated with fluorescence lifetime τ_i such that $\sum \alpha_i = 1$. The reliability of fitting was checked by numerical value of reduced chi-square (χ^2), Durbin–Watson (DW) parameter and also by visual inspection of residual distribution in the whole fitting range [30].

Molecular Docking

Molecular docking calculations were carried out using Autodock Vina software [31]. The input parameters for the proteins and the drug were followed in the similar way described earlier [32]. In brief, SDZ structure was obtained from NCBI database (PubChem compound CID 5215). The input parameters for the protein structures were downloaded from the RCSB Protein Data Bank (http://www.rcsb.org); PDB ID for the BSA, HSA and LYS were 3V03, 1AO6 and 2LYZ, respectively. The UCSF Chimera program (http://www.cgl.ucsf.edu/chimera) was used to prepare the structures for input by adding Gasteiger charges and running an energy minimization using steepest descent method with the generalized amber force field. The UCSF Chimera program was also used to remove co-crystallized ligands, crystal waters and other hetero-atoms (if any) before minimization. AutoDockTools (ADT) version 1.5.4 was used to add polar hydrogens to all the protein structures and saved in PDBQT file format, for input into AutoDock Vina version 1.0.3 (http://vina.scripps.edu). For the albumins (BSA & HSA), the search space was defined as a cube 60 Å on each side; whereas for LYS, the search space was a box with XYZ dimensions of 30 Å×30 Å×30 Å, respectively. Both the search space dimensions encompass the entirety of the proteins, as is required for blind docking. The AutoDock Vina parameter "Exhaustiveness", which determines how comprehensively the program searches for the lowest energy conformation, was set to the default value, eight, for all the docking setups. Once the blind docking technique was validated, the search spaces were decreased to encompass only the ligand binding sites in albumins within 20 Å×20 Å×20 Å volume space. The most favorable docked structure of the protein-ligand complex was viewed and handled with PyMol software.

Results and Discussion

Quenching of trp Fluorescence in Presence of Sulphadiazine

Intrinsic trp fluorescence of BSA, HSA as well as LYS appears at 340, 350 and 338 nm, respectively. In all the cases, the fluorescence intensity is quenched regularly with the addition of SDZ. Figure 1 shows a representative example of the fluorescence emission spectra of BSA titrated with different concentrations of SDZ in pH 7.4 buffer solutions. Comparison of the normalized fluorescence curves (data not shown) show no apparent difference in spectral position and width, even on highest concentration of SDZ addition in the respective cases while comparing with the protein fluorescence in absence of any SDZ.

A number of different processes may be responsible towards the quenching of fluorescence, such as, excited state reaction, molecular rearrangement, collisional quenching and also the ground state complex formation [33, 34]. Depending on the chemical nature of both the quenching agent and the

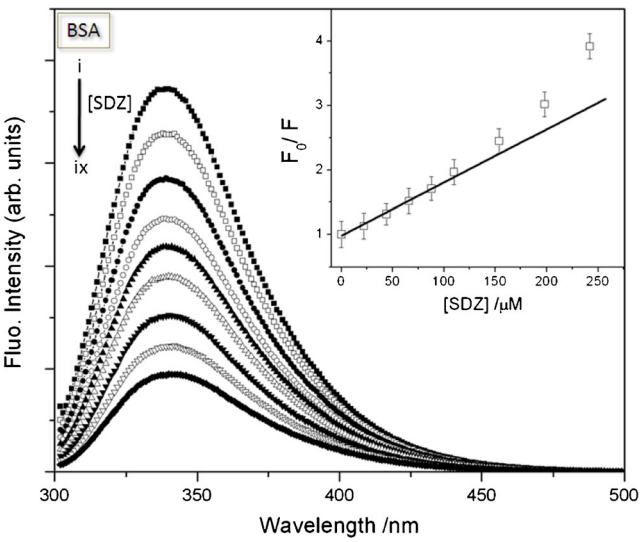

Fig. 1 Variation of trp fluorescence intensity of BSA with increasing concentrations of SDZ. [SDZ]/μM=0(i), 22(ii), 44(iii), 66(iv), 88(v), 110(vi), 154 (vii), 198 (viii), 242 (ix). Concentration of protein was kept fixed at 12 μM

chromophore, a broad distinction can be made between two forms of quenching: static and dynamic quenching. Static quenching results from the formation of a non-fluorescent fluorophore-quencher complex, formed in the ground state. Characteristic for this type of quenching is that increasing quencher concentration decreases the fluorescence intensity or quantum yield but does not affect the fluorescence lifetime. On the other hand, if the quenchers act by competing with the radiative deactivation process (e.g. through collisions), the ratio of the quantum yield in the absence, ϕ_0 and the presence, ϕ (or the fluorescence intensity F_0 and F, respectively), of the quencher will be equal to the ratio of the corresponding lifetimes, τ_0/τ. Nevertheless, the analysis of the quenching data is normally done by classical Stern-Volmer (SV) relations given in Eqs. (3) and (4) for the dynamic and static quenching cases, respectively [33].

$$\frac{\phi_0}{\phi} = \frac{F_0}{F} = \frac{\tau_0}{\tau} = 1 + K_{SV}[Q] = 1 + k_q\tau_0[Q] \quad (3)$$

$$\frac{\phi_0}{\phi} = \frac{F_0}{F} = 1 + K_S[Q]; \frac{\tau_0}{\tau} = 1 \quad (4)$$

Here, K_{SV} represents the Stern-Volmer quenching constant, k_q is diffusion controlled rate constant for bimolecular quenching, and [Q] is the quencher concentration. In the static quenching case, K_S is association constant for the fluorophore-quencher complex. In the inset of Fig. 1, the variation of F_0/F with SDZ concentration is also shown. Interestingly, the SV plot is linear till [SDZ] ~100 μM and shows deviation from linearity and moves upward beyond this concentration in all the proteins. The linear fitting of the quenching data in the lower concentration regime is shown by the solid line in the inset of Fig. 1. Interestingly, the fluorescence quenching behavior and the deviation from linearity remains identical for all the proteins within the experimental temperature range of 298–323 K. The magnitude of SV quenching constant (K_{SV}) obtained from the slope of this linear plot is listed in Table 1 for all the proteins. While the value of K_{SV} is found to be almost constant over the whole temperature range for albumins (BSA & HSA), there is a slight decrease in the corresponding value for LYS with increase in temperature ($K_{SV}/10^3$, M^{-1}=17.6 and 12.1 at 298 and 323 K, respectively). The decrease in K_{SV} at higher temperature indicates that the additional quenching mechanism responsible for the upward curvature (see below) in the SV plot is significant at higher concentration of SDZ for LYS in comparison with BSA and/or HSA. Before we discuss more about the origin of the upward curvature in SV plot, it is worth noting the effect of SDZ addition on the intrinsic trp fluorescence lifetime of the three proteins.

Analysis of trp Fluorescence Lifetime in Presence of Sulphadiazine

Figure 2 shows the time-resolved data of trp fluorescence decay for HSA and LYS obtained by exciting the sample at 295 nm and monitoring the fluorescence at the respective emission maximum. The corresponding data for BSA is almost identical to that of HSA. It is seen that in all the three cases, the experimental data needs more than one exponential fit to give acceptable statistical parameters. The decay times and the corresponding amplitude contributions for the two exponential fitting in BSA and HSA are 2.53 ns (74 %), 6.55 ns (26 %) and 3.43 ns (71 %), 6.67 ns (29 %), respectively. On the other hand for LYS, minimum three exponential decay function was necessary for adequate fitting of the experimental decay data. The corresponding fitting parameters are 0.77 ns (67 %), 2.11 ns (31 %) and 4.5 ns (3 %). The nature of the fluorescence decay and also the experimentally obtained parameters are consistent with the literature reported values [35–38]. Nevertheless, the measured decay represents the radiative relaxation process of trp fluorophore(s) for these systems and difference in the fluorescence decay time indicates the difference in location of the trp residue(s) in the protein structure. The origin of the multiple fluorescence decay times, even for proteins containing single trp residue, like in HSA, has attracted considerable attention since almost four decades ago [39, 40] and till continues to be a topic of intense research activities [41]. It is now more or less accepted that the multi-exponential trp fluorescence decay is mainly the outcome of fluorophore heterogeneity resulting from the

Table 1 Quenching constants (K_{SV}) for the linear part of the Stern-Volmer plot at different temperatures for BSA, HSA and LYS[a]

Temperature (K)	BSA			HSA			LYS		
	K_{SV}	S.D.	R	K_{SV}	S.D.	R	K_{SV}	S.D.	R
298	8.76±0.41	0.03	0.99	8.69±0.37	0.02	0.99	17.59±1.3	0.12	0.99
303	9.18±0.37	0.03	0.99	8.75±0.17	0.02	0.99	18.62±1.1	0.12	0.99
308	8.87±0.37	0.03	0.98	8.76±0.24	0.01	0.98	16.07±0.66	0.07	0.99
313	8.91±0.45	0.04	0.99	8.95±0.25	0.02	0.99	15.56±0.52	0.05	0.99
318	8.86±0.45	0.04	0.98	8.90±0.24	0.02	0.98	14.50±0.45	0.04	0.99
323	9.00±0.41	0.03	0.98	9.02±0.28	0.02	0.98	12.12±0.85	0.07	0.99

[a] K_{SV} values are represented in the unit of 10^3 M^{-1}, the error limit indicates the confidence interval in three independent measurements; Standard deviation (S.D.) and correlation coefficient (R) is also given in each case

formation of several microstates and is related to either a rotamer [42, 43] or an exciplex model [44]. Nevertheless, the average fluorophore lifetime (τ_{av}) can be expressed in terms of fractional contribution (f_i) of each decay time to the steady state intensity [30] as

$$\tau_{av} = \sum\nolimits_i f_i \tau_i = \frac{\sum_i \alpha_i \tau_i^2}{\sum_i a_i \tau_i} \quad (5)$$

We have calculated the τ_{av} from the measured fluorescence decay data in all the three proteins with different concentrations of SDZ. It was found that τ_{av} practically remains constant (τ_{av}=4.53, 4.82 and 1.9 ns for BSA, HSA and LYS, respectively) over the whole range of quencher concentration (Fig. 3). The detail tabulation of the fluorescence decay data in each quencher concentration for all three proteins is given in Table 2. The non-variance of fluorescence decay data confirms the static quenching mechanism in all these cases. Therefore, the slope obtained from the linear fitting of the low quencher concentration data (inset of Fig. 1) is representative of K_S as obtained from Eq. (4).

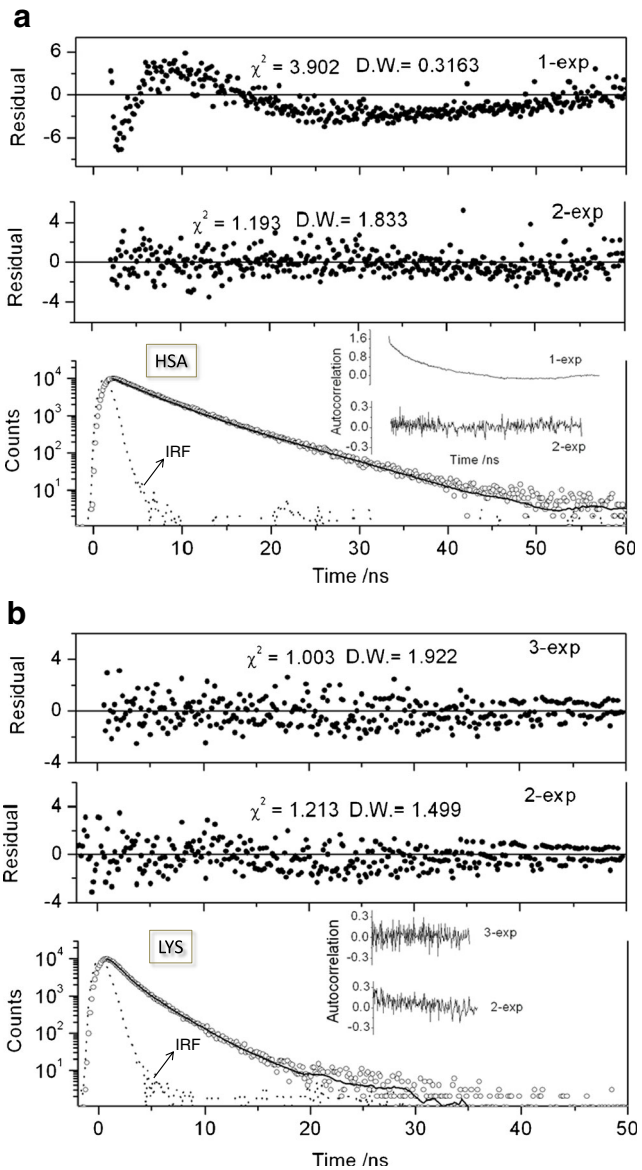

Fig. 2 Time-resolved fluorescence decay traces (*open circle*) of HSA (**a**) and LYS (**b**) in buffer solution of pH 7.4 along with the fitting data (*solid line*) and instrument response function (IRF) (λ_{exc}=295 nm). Distribution of weighted residual and autocorrelation function as well as numerical values of reduced chi-square (χ^2) and Durbin-Watson (D.W.) parameter is also shown for different fitting functions

Upward Curvature in S-V Plots

Positive deviations in SV plot of trp fluorescence quenching suggests the involvement of additional quenching process at higher concentration of SDZ. This additional mechanism may be related to the presence of a quenching sphere that diminishes the fraction of fluorescing molecules [45–48]. This model [45] assumes that, if the quencher is situated inside a spherical volume V adjacent to the fluorophore, an instantaneous quenching of the excited fluorophore by a quencher takes place without the need for diffusion-controlled collisional interaction (for dynamic quenching case) or the formation of a pure ground state complex (for static quenching mechanism). The probability for the quencher to be inside this volume at the time of excitation depends on the volume (V) itself and also on the quencher concentration, [Q]. The probability of this additional quenching, defined by the Poisson distribution, is introduced into the linear SV equation to give the following relations that describe all these quenching processes [45, 49].

$$\frac{F_0}{F} = \{1 + K_P[Q]\} \times e^{V_q \cdot [Q]} \quad (6)$$

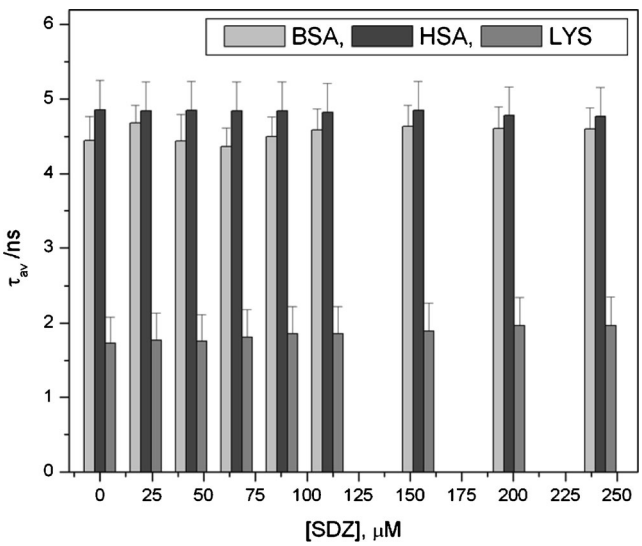

Fig. 3 Variation of average trp fluorescence decay time (τ_{av}) of BSA, HSA and LYS with increasing concentration of SDZ

Table 2 Fluorescence decay time (τ) of BSA, HSA and LYS titrated with different concentrations of SDZ. The excitation wavelength is 295 nm and the emission monitored at the respective fluorescence maxima.[a]

[SDZ], μM	BSA			HSA			LYS			
	τ_1 (a_1)	τ_2 (a_2)	τ_{av}	τ_1 (a_1)	τ_2 (a_2)	τ_{av}	τ_1 (a_1)	τ_2 (a_2)	τ_3 (a_3)	τ_{av}
0	2.5 (74)	6.5 (26)	4.4	3.4 (71)	6.7 (29)	4.9	0.8 (67)	2.1 (31)	4.0 (3)	1.7
22	2.3 (64)	6.2 (36)	4.7	3.6 (73)	6.7 (27)	4.8	0.8 (63)	2.1 (34)	4.1 (3)	1.8
44	2.5 (73)	6.5 (27)	4.4	3.6 (72)	6.6 (28)	4.9	0.7 (56)	1.8 (39)	3.6 (6)	1.8
66	2.4 (74)	6.4 (26)	4.4	3.8 (80)	7.0 (20)	4.8	0.8 (62)	2.1 (36)	4.7 (2)	1.8
88	2.6 (73)	6.5 (27)	4.5	3.7 (76)	6.8 (24)	4.8	1.1 (70)	2.4 (29)	4.8 (1)	1.9
110	3.1 (76)	6.7 (24)	4.6	3.8 (79)	6.9 (21)	4.9	0.9 (61)	2.2 (37)	4.4 (2)	1.9
154	3.1 (74)	6.6 (26)	4.6	3.9 (84)	7.3 (16)	4.7	0.9 (54)	2.0 (41)	4.0 (5)	1.9
198	3.2 (76)	6.7 (24)	4.6	4.0 (87)	7.5 (13)	4.8	1.2 (73)	2.6 (27)	6.6 (1)	2.0
242	3.4 (78)	6.8(22)	4.6	4.1 (88)	7.5 (12)	4.8	0.9 (51)	2.0 (43)	3.9 (6)	2.0

[a] The decay times (τ/ns) are within the error limit ±0.1 ns; the values in parenthesis are the corresponding amplitudes (in %); τ_{av} indicates the average lifetime (ns) calculated using Eq. (5)

$$V_q = N_A \times V = N_A \times \frac{4}{3}\pi R_S^3 \tag{7}$$

Here, K_P is quenching constant related to the linear portion of the SV plot and R_S is the radius of quenching sphere. The experimental data points are nicely fitted with the simulated curve using Eq. (6) as shown for different cases in figure 1S (a-c) of the supplementary material. The calculated value for the radius of the quenching sphere is ~10.4 Å and ~10.9 Å for HSA and BSA, respectively at 298 K. However, for LYS, the corresponding parameter is found to be ~12.0 Å. The values are somewhat greater than the sum of the estimated radii of the trp (fluorophore) and SDZ (quencher) molecule. However, it is already reported in the literature that the quenching partners not necessarily to be in close contact for the quenching sphere model to operate [49]. This is due to the fact that once the quencher is inside the sphere it can diffuse through the distance separating the fluorophore and the quencher during excitation and still show the transient effect. Interestingly, the magnitude of R_S increases about 10 % with change in temperature from 298 K to 318 K. This observation is consistent if it is hypothesized that with increase in temperature, the quencher can cover even a longer distance to show the transient effect.

Binding Constants and Number of Binding Sites

For static quenching, we can deduce the binding constant (K) resulting from the formation of ground state complex between fluorophore and the quencher. As discussed before the intrinsic tryptophan fluorescence quenching of the proteins by SDZ follow mostly static type of interaction, we can deduce the binding constant (K) which is calculated by using the following method.

If there are similar and independent binding sites present in the macromolecular host molecules (M), then the binding of SDZ (quencher, Q) can be described by the following equilibrium [50]:

$$M + nQ \rightleftharpoons M.....Q_n \tag{8}$$

M….Q_n is the complex between the fluorophore and the quencher. The apparent binding or association constant is given by

$$K = \frac{[M.....Q_n]}{[M] \times [Q]^n} \tag{9}$$

If the overall amount of bio-macromolecule (bound and unbound) is $[M]_0$, then $[M]_0 = [M....Q_n] + [M]$. Given that $[M]/[M]_0 = F/F_0$, we can write

$$log\left[\frac{F_0 - F}{F}\right] = \log K + n log[Q] \tag{10}$$

From the slope and intercept of the simulated linear plot using the above equation, the binding constant, K and number of binding sites, n can be obtained for different protein/SDZ combination at various temperatures. The corresponding values are displayed in Table 3. The representative plots for all the three proteins at different temperatures are displayed in supplementary section (Figs. 2S, 3S and 4S).

The binding constant value ($K/10^4$ M^{-1}) for HSA, BSA and LYS with SDZ are found to be approximately 3.6, 4.2 and 20.1, respectively. The magnitude of n in case of albumins varies within the range 1.15±0.05. Efficient quenching of trp fluorescence in presence of the drug clearly indicates a strong

Table 3 Association constant (K) and number of binding sites (n) obtained from the double-log plot of interaction of SDZ with BSA, HSA and LYS at different temperatures[a]

Temp	BSA				HSA				LYS			
	K	n	S.D.	R	K	n	S.D.	R	K	n	S.D.	R
298	4.23	1.2	0.02	0.99	3.57	1.2	0.03	0.99	20.12	1.3	0.12	0.99
303	4.99	1.1	0.03	0.99	4.06	1.1	0.03	0.99	29.84	1.3	0.12	0.99
308	6.60	1.2	0.03	0.99	3.57	1.1	0.04	0.98	47.03	1.4	0.07	0.99
313	9.85	1.2	0.03	0.99	4.19	1.1	0.05	0.99	45.49	1.4	0.05	0.99
318	11.93	1.2	0.02	0.99	4.46	1.1	0.04	0.99	64.41	1.4	0.04	0.99
323	14.65	1.2	0.03	0.99	5.00	1.1	0.04	0.99	89.71	1.5	0.07	0.99

[a] K values are represented in the unit of 10^4 M^{-1}; Standard deviation (S.D.) and correlation coefficient (R) is also given in each case

interaction between trp and SDZ of all the proteins. In the albumins, trp-214 is located in sub-domain IIA, which is a well-characterized binding cavity for small organic molecules. Also, it indicates that SDZ interact with trp-214 only. In case of BSA, although it contains two tryptophan molecules, the other tryptophan residue (trp-134, located in domain – I) remains inaccessible to the water soluble ligands. On the other hand, relatively higher value of n (1.40±0.10) in case LYS indicates mutual interaction from both the trp residues (trp62 and trp108) in the ligand binding site with SDZ. It is interesting to note the variation of K value with increase in temperature for the three different proteins (Table 3). While the magnitude of K in HSA increases only by a factor of ~1.4 by increasing the temperature from 298 K to 323 K, the corresponding increase is ~3.5 and ~4.5 times in the cases of BSA and LYS, respectively. As discussed above, both BSA and LYS contains multiple trp residues in the binding cavity in contrast to a single trp residue for HSA. The difference in the increase in K values in the former cases can be regarded as due to some positive cooperative effect in the binding process at elevated temperature. Similar observation was also reported recently [27], where it was shown that the chemiluminescent probe luminol binds cooperatively only in the ligand binding domain of BSA but not in HSA.

Thermodynamics of Protein-SDZ Interaction: Nature of Forces Responsible for the Association

The interaction forces between drugs and bio-molecules may include electrostatic interactions, formation of multiple hydrogen bonds, van der Waals interaction, hydrophobic and steric contacts within the antibody binding site etc. [51]. The sign and magnitude of the thermodynamic parameters can account for the main factor(s) responsible towards the stability of drug—protein complex [52]. In order to elucidate the nature of the binding interaction of SDZ with proteins, the thermodynamic parameters were calculated using van't Hoff relation [53]. Assuming the change in enthalpy (ΔH) for the protein-ligand binding process to be insignificant over the temperature range studied, the association constant (K) and the change in other thermodynamic parameters with temperature can be written by following relations:

$$logK = \frac{\Delta S}{2.303R} - \frac{\Delta H}{2.303RT} \tag{11}$$

$$\Delta G = \Delta H - T.\Delta S \tag{12}$$

The enthalpy (ΔH) and entropy (ΔS) change was calculated from the slope and intercept of the van't Hoff plot at six different temperatures, within 298 to 323 K range; whereas, Gibb's free energy change (ΔG) can be estimated from Eq. (12). The representative plots are shown in Fig. 4 and all the thermodynamic parameters are collected in Table 4.

The negative value of the free energy change (ΔG) is indicative of a spontaneous binding of these ligands to the proteins. Further, this exothermic process is accompanied by positive ΔS values in all the cases. A positive ΔS value is often indicative of a hydrophobic mechanism in drug—protein interaction [52]. Specific electrostatic interaction among

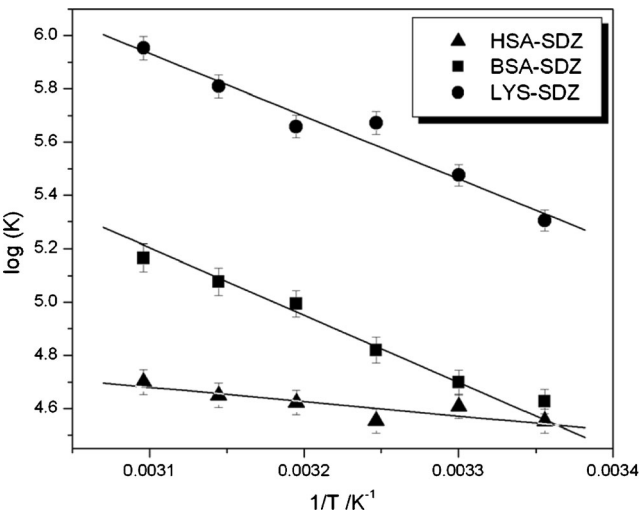

Fig. 4 van't Hoff plot for the binding of SDZ with BSA, HSA and LYS

Table 4 Relative thermodynamic parameters for the interaction of SDZ with BSA, HSA and LYS[a]

Temp	BSA			HSA			LYS		
	ΔG	ΔH	ΔS	ΔG	ΔH	ΔS	ΔG	ΔH	ΔS
298	−26.0±0.2	48.4±4.1	0.25±0.01	−26.0±0.3	10.3±0.2	0.12±0.01	−30.4±0.3	45.1±5.8	0.25±0.01
303	−27.2±0.1			−26.6±0.2			−31.7±0.2		
308	−28.5±0.1			−27.2±0.1			−32.9±0.1		
313	−29.8±0.1			−27.8±0.2			−34.2±0.1		
318	−31.0±0.1			−28.4±0.1			−35.5±0.1		
323	−32.2±0.2			−29.1±0.2			−36.8±0.2		

[a] Gibb's free energy (ΔG) and enthalpy (ΔH) changes are given in kJ mol^{-1} and entropy (ΔS) change is given in kJ mol^{-1} K^{-1}

ionic species in solution is characterized by positive ΔS and negative ΔH values; whereas, negative entropy and enthalpy changes indicate the importance of van der Waals force as well as hydrogen bond formation. From the results displayed in Table 4, it is clear that the hydrophobic interaction plays the major role in SDZ binding in all the cases. Interestingly, the net entropy change in the case of BSA and LYS is almost twice than that in HSA. This may be due to the fact that the binding in HSA is mostly in the single binding site (domain IIA) and the resulting interaction is due to the presence of only one trp in the protein. Recent report on the interaction of sodium sufadiazine with HSA also predicts the involvement of sub-domain IIA as the principal binding region [54]. However, in case of both the BSA and LYS, the interaction is stronger due to the presence and involvement of more than one trp sites with the drug molecule. The present argument is also manifested in lower values of the binding constant (K), number of binding sites (n) and free energy change (ΔG) in HSA (Tables 3 and 4) in comparison with BSA and LYS. Nevertheless, the whole binding process is considered as entropy driven in all the cases and the increase in entropy due to the ligand binding might be due to the destruction of the protein secondary structure.

Molecular Docking Studies

The best energy ranked results of SDZ binding with BSA and LYS are shown in Fig. 5. The binding result for HSA and the orientation of the drug (SDZ) is quite similar to that in case of BSA. The modeling results suggested that SDZ interacts with both the albumins (BSA & HSA) at site I in subdomain IIA, and the interaction between them was mainly dominated by a hydrophobic force, which was in agreement with the binding mode proposed in thermodynamic analysis. Furthermore, the docking results show that the location of SDZ is ~10.8 Å from the trp214 in HSA (for BSA, it is ~10.1 Å from trp213); whereas, the distance ranges within 4.1~6.7 Å from the three trp residues in the binding site of LYS. These results provide a good structural basis to explain the fluorescence quenching of the proteins in presence of SDZ and in nice agreement with the calculated distance parameters from the Stern-Volmer plots,

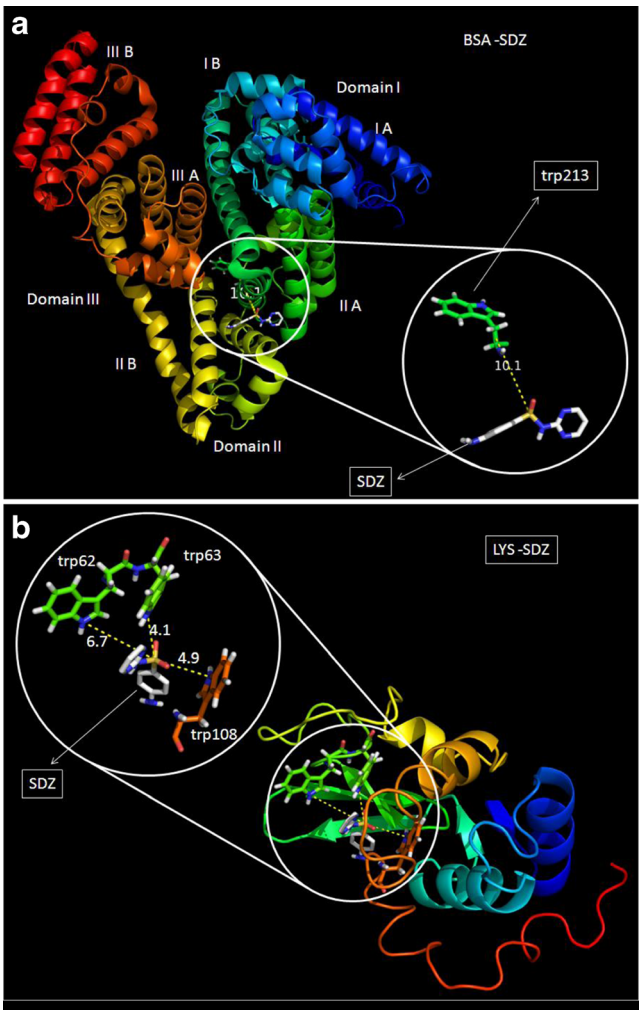

Fig. 5 Minimum energy docking structure of SDZ with BSA (**a**) and LYS (**b**). The zoomed representation of the orientation of the drug (SDZ) and the distance (Å) from the tryptophan (trp) residues in the binding site is also given in each case

particularly for albumins. However for LYS, the difference between the experimental and calculation data indicates a more complex nature of interaction between the fluorophore and SDZ, possibly due to the presence of three tryptophan moieties in close vicinity at the binding site. Nevertheless, the free energy change of binding (ΔG) obtained from the docking simulations was −29.9, −30.5 and −27.6 kJ mol^{-1}, for BSA, HSA and LYS respectively which are in good agreement with the experimentally obtained values. The little difference between these two results may be due to exclusion of solvent in docking simulations and/or rigidity of the receptor other than tryptophan.

Conclusions

The interaction between model water soluble proteins like bovine and human serum albumins (BSA and HSA, respectively) and lysozyme (LYS) with sulfadiazine (SDZ) were studied by monitoring the intrinsic tryptophan fluorescence quenching of proteins in presence of the ligand at different temperatures. The results show that the binding pattern of SDZ is similar in all the proteins indicating a preferential interaction at the hydrophobic sites of protein residue. The binding interaction is relatively strong with an apparent association constant ~10^4 M^{-1} and responsible for the efficient trp fluorescence quenching. Estimation of thermodynamic parameters indicates that the spontaneous complexation occurs through an entropy driven pathway. The structural basis of fluorescence quenching and the calculated thermodynamic parameters were corroborated with molecular docking calculation results. The knowledge of interaction can lead to better understanding of the mechanism of sulfonamide related reaction in warm blooded animals and also binding as well as transport properties of these model proteins toward the widely used anti-bacterial drug like SDZ at the molecular level.

Acknowledgement Financial support from Council of Scientific and Industrial Research (CSIR), Govt. of India through a research project 01(2568)/12-EMR-II is gratefully acknowledged. Thanks are also due to Department of Science & Technology (DST), Govt. of India for supporting the Chemistry Department through FIST program.

References

1. Rogers KS, Lees GE, Simpson RB (1988) Effects of single-dose and three-day trimethoprim-sulfadiazine and amikacin treatment of induced Escherichia coli urinary tract infections in dogs. Am J Vet Res 49:345–349
2. Genç Y, Özkanca R, Bekdemir Y (2008) Antimicrobial activity of some sulfonamide derivatives on clinical isolates of staphylococus aureus. Ann Clin Microbiol Antimicrob 7:17–22
3. Council Directive (1996) 96/23/EC of 29 April 1996, Brussels
4. Commission Regulation (EC, 1996) No 281/96 of 14 February 1996, Brussels
5. Mauri-Hellweg D, Bettens F, Mauri D, Brander C, Hunziker T, Pichler JW (1995) Activation of drug-specific CD4+ and CD8+ T cells in individuals allergic to sulfonamides, phenytoin, and carbamazepine. J Immunol 155:462–472
6. Gamba V, Terzano C, Fioroni L, Moretti S, Dusi G, Galarini R (2009) Development and validation of a confirmatory method for the determination of sulphonamides in milk by liquid chromatography with diode array detection. Anal Chim Acta 637:18–23
7. Olson RE, Christ DD (1996) Plasma protein binding of drugs. Ann Rep Med Chem 31:327–336
8. Fasano M, Curry S, Terreno E, Galliano M, Fanali G, Narciso P, Notari S, Ascenzi P (2005) The extraordinary ligand binding properties of human serum albumin. IUBMB Life 57:787–796
9. Kragh-Hansen U, Chuang VTG, Otagiri M (2002) Practical aspects of the ligand-binding and enzymatic properties of human serum albumin. Biol Pharm Bull 25:695–704
10. Dockal M, Carter DC, Ruker F (2000) Conformational transitions of the three recombinant domains of human serum albumin depending on pH. J Biol Chem 275:3042–3050
11. Hu YJ, Liu Y, Zhao RM, Dong JX, Qu SS (2006) Spectroscopic studies on the interaction between methylene blue and bovine serum albumin. J Photochem Photobiol A: Chem 179:324–329
12. Zhou B, Qi ZD, Xiao Q, Dong JX, Zhang YZ, Liu Y (2007) Interaction of loratadine with serum albumins studied by fluorescence quenching method. J Biochem Biophys Methods 70: 743–747
13. Valanciunaite J, Bagdonas S, Streckyte G, Rotomskis R (2006) Spectroscopic study of TPPS4 nanostructures in the presence of bovine serum albumin. Photochem Photobiol Sci 5:381–388
14. Hansen UK (1981) Molecular aspects of ligand binding to serum albumin. Pharmacol Rev 33:17–53
15. He XM, Carter DC (1992) Atomic structure and chemistry of human serum albumin. Nature 358:209–215
16. Redfield C, Dobson CM (1990) 1H NMR studies of human lysozyme: spectral assignment and comparison with hen lysozyme. Biochemistry 29:7201–7214
17. Parrot JL, Nicot G (1963) Antihistaminic action of lysozyme. Nature 197:496–496
18. Huang SL, Maiorov V, Huang PL, Ng A, Lee HC, Chang YT, Kallenbach N, Huang PL, Chen HC (2005) Structural and functional modeling of human lysozyme reveals a unique nanopeptide, HL9, with anti-HIV activity. Biochemistry 44:4648–4655
19. Huang SL, Huang PL, Sun YT, Huang PL, Kung HF, Blithe DL, Chen HC (1999) Lysozyme and RNases as anti-HIV components in β-core preparations of human chorionic gonadotropin. Proc Natl Acad Sci U S A 96:2678–2681
20. Mine Y, Ma FP, Lauriau S (2004) Antimicrobial peptides released by enzymatic hydrolysis of hen egg white lysozyme. J Agric Food Chem 52:1088–1094
21. Gorbenko GP, Loffe VM, Kinnunen PKJ (2007) Binding of lysozyme to phospholipid bilayers: evidence for protein aggregation upon membrane association. Biophys J 93:140–153
22. Gu Z, Zhu X, Ni S, Su Z, Zhou HM (2004) Conformational changes of lysozyme refolding intermediates and implications for aggregation and renaturation. Int J Biochem Cell 36:795–805
23. Fang Y, Yi L, Fang Y (2003) Unfolding of lysozyme induced by urea and guanidine hydrochloride studied by "phase diagram" method of fluorescence. Acta Chim Sinica 61:803–807
24. Yue QL, Song ZH, Dong FX (2008) A study on photochemical behavior of lysozyme-bromophenol blue complex and its analytical application. Spectrochim Acta 69A:1097–1102
25. Sheng CJ, Dian HD (1982) Lysozyme, Shandong Science and Technology Press, p 50–51

26. Imoto T, Foster LS, Ruoley JA, Tanaka F (1972) Fluorescence of lysozyme: emissions from tryptophan residues 62 and 108 and energy migration. Natl Acad Sci USA 69:1151–1155
27. Moyon NS, Mitra S (2011) Luminol fluorescence quenching in biomimicking environments: sequestration of fluorophore in hydrophobic domain. J Phys Chem B 115:10163–10172
28. Phukan S, Mitra S (2012) Fluorescence behavior of ethidium bromide in homogeneous solvents and in presence of bile acid hosts. J Photochem Photobiol A: Chem 244:9–17
29. Bevington PR (1969) Data reduction and error analysis for the physical sciences. McGraw-Hill, New-York
30. Lakowicz JR (2006) Principles of fluorescence spectroscopy, 3rd edn. Springer, Singapore, Chapter 4
31. Trott O, Olson AJ (2010) AutoDock Vina: improving the speed and accuracy of docking with a new scoring function, efficient optimization, and multithreading. J Comput Chem 31:455–461
32. Bieganski RM, Yarmush ML (2011) Novel ligands that target the mitochondrial membrane protein mitoNEET. J Mol Graphics Modell 29:965–973
33. Valeur B (2002) Molecular fluorescence principles and applications. Wiley-VCH, Weinheim
34. Eftnik MR (2002) In: Lakowicz JR (ed) Topics in fluorescence spectroscopy principles, vol 2. Plenum Press, NY, pp 53–126
35. Yamashita S, Nishimoto E, Szabo AG, Yamasaki N (1996) Steady-state and time-resolved fluorescence studies on the ligand-induced conformational change in an active lysozyme derivative, kyn62-lysozyme. Biochemistry 35:531–537
36. Nishimoto E, Yamashita S, Yamasaki N, Imoto T (1999) Resolution and characterization of tryptophenyl fluorescence of hen egg-white lysozyme by quenching- and time- resolved spectroscopy. Biosci, Biotechnol, Biochem 63:329–336
37. Jha NS, Kishore N (2009) Binding of streptomycin with bovine serum albumin: energetics and conformational aspects. Thermochim Acta 482:21–29
38. Mishra B, Barik A, Priyadarsini KI, Mohan H (2005) Fluorescence spectroscopic studies on binding of a flavonoid antioxidant quercetin to serum albumins. J Chem Sci 117:641–647
39. Beechem JM, Brand L (1985) Time-resolved fluorescence in proteins. Annu Rev Biochem 54:43–71
40. Swaminathan R, Krishnamoorthy G, Periasamy N (1994) Similarity of fluorescence lifetime distributions for single tryptophan proteins in the random coil state. Biophys J 67:2013–2023
41. Albani JR (2007) New insights in the interpretation of tryptophan fluorescence. J Fluoresc 17:406–417
42. Szabo G, Rayner DM (1980) Fluorescence decay of tryptophan conformers in aqueous solution. J Am Chem Soc 102: 554–563
43. Ross JBA, Wyssbrod HR, Porter RA, Schwartz GP, Michaels CA, Laws WR (1992) Correlation of tryptophan fluorescence intensity decay parameters with 'H NMR-determined rotamer conformations: [tryptophan]2oxytocin. Biochem 31:1585–1594
44. Vekshin N, Vincent M, Gallay J (1992) Excited-state lifetime distributions of tryptophan fluorescence in polar solutions. Evidence for solvent exciplex formation. Chem Phys Lett 199:459–464
45. Eftink MR, Ghiron CA (1976) Fluorescence quenching of indole and model micelle systems. J Phys Chem 80:486–493
46. Birks JB, Georghiout S (1968) Energy transfer in organic systems VII. Effect of diffusion on fluorescence decay. J Phys B At Mol Phys 1:958–965
47. Jin B, Min KS, Han SW, Kim SK (2009) DNA-binding geometry dependent energy transfer from 4′,6-diamidino-2-phenylindole to cationic porphyrins. Biophys Chem 144:38–45
48. Airinei A, Tigoianu RI, Rusu E, Dorohoi DO (2011) Fluorescence quenching of anthracene by nitroaromatic compounds. Digest J Nanomater Biostruct 6:1265–1272
49. Castanho MARB, Prieto MJE (1998) Fluorescence quenching data interpretation in biological systems: the use of microscopic models for data analysis and interpretation of complex systems. Biochim Biophys Acta 1373:1–16
50. Singh TS, Mitra S (2011) Interaction of cinnamic acid derivatives with serum albumins: a fluorescence spectroscopic study. Spectrochim Acta 78A:942–948
51. Leckband D (2000) Measuring the forces that control protein interactions. Annu Rev Biophys Biomol Struct 29:1–26
52. Ross PD, Subramanian S (1981) Thermodynamics of protein association reactions: forces contributing to stability. Biochemistry 20: 3096–3102
53. Silbey RJ, Alberty RA (2002) Physical chemistry, 3rth edn. Wiley, Singapore
54. Geng S, Liu G, Li W, Cui F (2013) Molecular interaction of ctDNA and HSA with sulfadiazine sodium by multispectroscopic methods and molecular modeling. Luminescence 28:785–792. doi:10.1002/bio.2457